



Photoconductive studies on electron beam evaporated CdSe films

K.R. Murali^{a,*}, K. Sivaramamoorthy^b, M. Kottaisamy^c, S. Asath Bahadur^d

^a Central Electrochemical Research Institute, Karaikudi 630 006, India

^b Department of Physics, Rajapalayam Raju's College, Rajapalayam, India

^c Department of Chemistry, Kalasalingam University, Krishnankoil, India

^d Department of Physics, Kalasalingam University, Krishnankoil, India

ARTICLE INFO

Article history:

Received 27 July 2008

Received in revised form

29 March 2009

Accepted 1 May 2009

Keywords:

Semiconductors

Thin films

II–VI

Electronic materials

ABSTRACT

Thin CdSe films were electron beam evaporated. The CdSe powder synthesized in the laboratory by a chemical method was used as source for the deposition of films. Clean glass and titanium substrates were used as substrates. The substrate temperature was varied in the range of 30–250 °C. X-ray diffraction studies indicated polycrystalline hexagonal structure. The band gap was 1.65 eV. The grain size was 15–30 nm with increase of substrate temperature. Photoconductive cells fabricated with the doped and undoped films have exhibited high photosensitivity and high signal to noise ratio. The current voltage characteristics were linear.

© 2009 Elsevier B.V. All rights reserved.

1. Introduction

In recent years much attention has been shown in semiconducting II–VI group compounds (CdSe, ZnSe, CdS, CdTe, etc.) because of their opto-electronic properties and applications. These materials have been synthesized by various techniques including spray pyrolysis, sol–gel, chemical bath deposition, electrodeposition, vacuum deposition, etc. [1–3]. Cadmium selenide is an important member of this group of binary compounds. It has a direct intrinsic band gap of 1.74 eV, which makes it an interesting material for various applications such as solar cells, photo-detector, light emitting diodes and other opto-electronic devices [4–6]. Shreekanthan et al. [7] found that CdSe films vacuum evaporated at room temperature are cadmium rich with segregated selenium globules, but a deposition at higher temperatures has been found to yield stoichiometric and homogeneous films. CdSe often possesses n-type conductivity in bulk as well as in thin films [8]. However, not enough studies are reported of the growth, characterization and properties of the material in its thin films form [9]. Recently, Hus et al. [10] have reported on the properties of thermal and electron beam evaporated CdSe films from commercial CdSe powder. The evaluation of any material for applications is complete and meaningful only when its structure and composition are precisely known and related to its electronic properties. In the present work, the properties of

electron beam CdSe films prepared using the laboratory synthesized CdSe powder are studied.

2. Experimental

High purity cadmium selenide powder has been prepared [11] by the reaction of aqueous solutions of cadmium acetate with sodium selenosulfate under optimum conditions of pH = 10, obtained by the addition of ammonium hydroxide. Normally selenium dissolves in hot aqueous solutions of alkali metal sulfites yielding alkali selenosulfate or selenosulfites. Selenosulfate is stable under high alkaline conditions (pH = 10). As the pH is decreased gradually below 5.5, selenium is precipitated out. This selenium reacts with the cadmium ions to yield cadmium selenide.

About 30 g of pure selenium powder was washed with distilled water and degreased with trichloroethylene or acetone. Sodium sulfite of 235 g was added and heated up to 95 °C and allowed to remain for 20 h. The solution was filtered till it was ensured that no more selenium separated out. The solution was allowed to age for 20 h. Cadmium acetate of 34 g was dissolved in 250 ml of triple distilled water. This solution was kept in a 3 l pyrex round bottomed flask fitted with ground joints. Ammonia of 100 ml was added to obtain a clear solution. Selenosulfate solution of 250 ml was mixed with 30 ml of ammonia and added to the cadmium ammonia complex in the flask and slowly refluxed over an electric heating mantle. The solution was initially yellow which slowly turned to orange red with tiny crystals of CdSe floating on the

* Corresponding author. Tel.: +91 4565 227550; fax: +91 456 227553.
E-mail address: muraliramkrish@gmail.com (K.R. Murali).

surface of the solution along the sides of the flask. The remaining selenosulfate solution was added and refluxing continued for 4 h when the precipitate turned into shiny black color. The precipitate was kept for 20 h and then filtered through a Whatmann filter paper using a Buchner funnel with vacuum suction arrangement. Thus obtained precipitate was thoroughly mixed with hot solution of sodium sulfite to remove any trace of selenium. Washing with distilled water was continued till the filtrate was free from sulfite. To remove traces of cadmium oxide, the precipitate was washed with hot acetic acid solution (70 °C). Further washing with distilled water was continued till the pH of the filtrate was found to be neutral. Purified ethanol was employed for final washing to remove moisture. The precipitate was dried in a vacuum oven. Thus prepared CdSe powder has been annealed at 300 °C in argon atmosphere for 20 min. This ensured the complete removal of excess selenium. The powders were stored in a vacuum desiccator.

Thin CdSe films were deposited using a Hind Hivac coating unit. A vacuum better than 8×10^{-6} Torr was used during evaporation. The source substrate distance was maintained as 15 cm. The CdSe powder synthesized in the laboratory was used for the deposition of films. Clean glass and titanium substrates were used as substrates. The substrate temperature was varied in the range of 30–250 °C. Indium ohmic contacts were provided on the edges of the surface of the films for photoconductivity measurements. A 250 W tungsten halogen lamp was used for photoconductivity measurements. Spectral response measurements were made using photophysics monochromator.

Copper doping was done by dipping the films in CuCl_2 solution of different concentrations in the range of 0.001–0.011 M. After dipping the films were annealed in air at 450 °C for 10 min.

Noise characteristics of the doped and undoped photoconductive films were studied as follows. The load resistance was adjusted to a value equal to the resistance of the photoconductive film. The power supply was switched ON and in the absence of an applied bias voltage, the signal across the cell was measured; this represents the noise signal due to the power supply. Next the chopper was switched ON and maintaining the light in the OFF condition, the signal was measured across the cell. This value gives the total noise signal due to chopper and power supply. After this, the light was switched ON, this causes the resistance of the film to decrease, when light is incident on the cell, this causes an increase in voltage drop across the load resistance. The AC signal across the cell on illumination is measured and the signal to noise ratio (S/N ratio) is calculated from the signal and noise signal values.

3. Results and discussion

Atomic absorption spectrometry was used to determine the purity of the powder. The purity of the synthesized powder was comparable to the commercially available AR grade Koch light powder (Table 1). The content of Cd and Se is 52% and 48%, respectively.

X-ray diffractograms (XRD) of the as-prepared and annealed CdSe powders exhibit all reflections corresponding to single phase

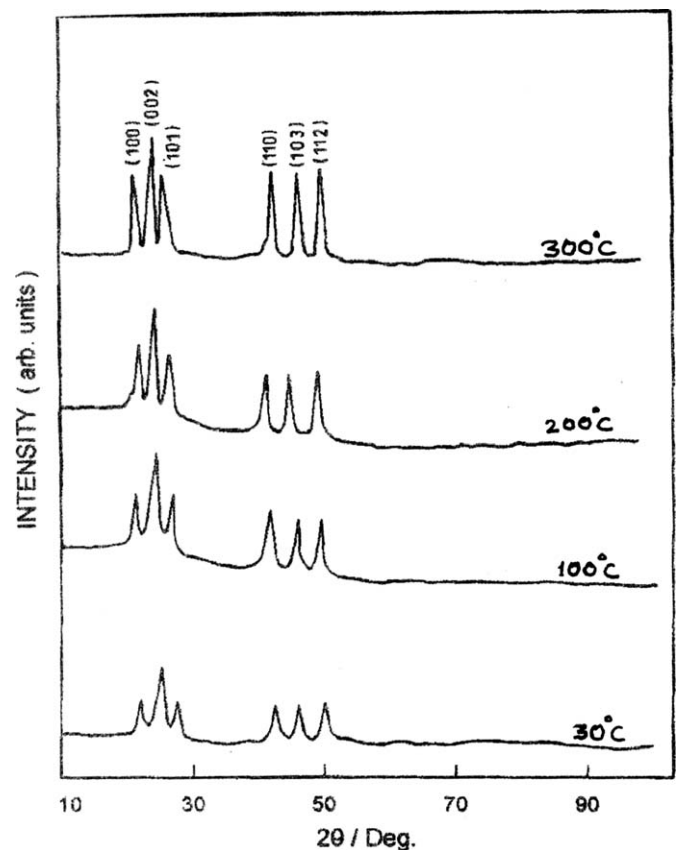


Fig. 1. XRD patterns of CdSe films deposited at different substrate temperatures.

hexagonal CdSe. Fig. 1 shows the XRD pattern of the CdSe films deposited at different substrate temperatures. The as deposited films were polycrystalline in nature possessing the hexagonal structure. Mixed cubic and hexagonal phases were not observed like Hus et al. [10]. As the substrate temperature increased from 30 to 250 °C, the peaks became sharper and increased in intensity. This indicates that the crystallinity improves with increase of substrate temperature. The lattice parameters were determined from the XRD data. The lattice constants 'a' and 'c' were 4.31 and 7.05 Å. These values are in good agreement with the literature values.

The structural parameters, such as lattice constant, internal stress and dislocation density, were calculated from the XRD data for CdSe films, and their variation as a function of substrate temperature was studied. The lattice parameter *a* for hexagonal CdSe film was calculated using the relation

$$1/d^2 = 4/3\{(h^2 + k^2 + l^2)/a^2\} + l^2/c^2$$

where *h*, *k*, *l* are the lattice planes and *d* is the interplanar spacing determined using Bragg's equation. The variation of the lattice constant with the deposition temperature is presented in Table 2. The lattice constant increased with substrate temperature. The change of lattice constant with substrate temperature clearly indicated that the crystallites were under stress, leading to either elongation or compression of the lattice constant. This might be due to the change of density and nature of native imperfections with the deposition temperature of the film [12]. In general, all polycrystalline thin films are in a state of stress irrespective of their preparation technique. The total stress present in the films is equal to the sum of thermal stress and intrinsic stress in the absence of applied external stress:

$$\sigma_{\text{total}} = \sigma_{\text{Thermal}} + \sigma_{\text{Intrinsic}}$$

Table 1
AAS analysis of CdSe powders.

Sample	Impurity content in ppm							
	Ti	Ca	K	Na	Zn	Pb	Co	As
CdSe (prepared)	10	65	2	–	–	3	–	–
CdSe (Koch light)	16	110	7	5	3	3	5	8

Table 2
Structural parameters of CdSe films.

Deposition temperature (°C)	Lattice parameters (Å)		Internal stress (GPa)	Dislocation density $\times 10^{15}$ (lines m^{-1})
	(a)	(c)		
30	4.51	7.42	−0.23	4.3
50	4.53	7.43	−0.16	2.8
70	4.55	7.45	−0.12	1.9
80	4.56	7.46	−0.07	0.6

The difference in thermal expansion coefficients of substrate and film gives rise to thermal stress, whereas the difference in lattice constant from that of bulk led to the development of intrinsic stress in the film. In our present study, the thermal stress is calculated using the following relation [13]:

$$\sigma_{\text{Thermal}} = (\alpha_{\text{CdSe}} - \alpha_{\text{titanium}})\Delta T Y$$

where α_{CdSe} ($7.434 \times 10^{-6}/^{\circ}\text{C}$) [14] and $\alpha_{\text{glass}} = 8.04 \times 10^{-6}/^{\circ}\text{C}$ are the thermal expansion coefficients of CdSe and titanium, respectively. Y is Young's modulus of CdSe and ΔT is the temperature of the CdSe film during the formation minus the temperature at measurement. The evaluated thermal stress was found to be compressive in nature, and varied in the range of 8–15% of the total stress with the increase of deposition temperature. It was reported that the thermal stress was approximately 5% of the total stress in the case of evaporated ZnSe films grown at higher temperatures [15]. Hence, it was assumed that for high melting point materials like ZnSe and ZnS, only internal stress would dominate over thermal stress. The internal stress in CdSe films was determined using the difference in lattice constants of the film and bulk material using the relation [16]

$$\sigma_{\text{Intrinsic}} = Y(a - a_0)/2\gamma a_0$$

Here, 'a' is the lattice constant measured from the XRD, a_0 is the bulk lattice constant and γ is Poisson's ratio. The variation of internal stress with deposition temperature is presented in Table 2.

The dislocation density (δ) was determined using the relation [15]

$$\delta = 15\beta \cos \theta / 4aD$$

The variation of dislocation density with substrate temperature is also indicated in Table 2. It was observed that the dislocation density decreased with the increase of deposition temperature. This might be due to the improvement in crystallinity.

Optical absorption studies were made on the films deposited at different substrate temperatures. An identical uncoated glass substrate was introduced in the reference beam to take care of the substrate absorption. Using the absorbance data (Fig. 2) recorded in the range of 300–800 nm, only one figure is presented since the absorbance spectra of all the films deposited at other substrate temperatures are identical. A plot of $(\alpha h\nu)^2$ vs $h\nu$ was linear; extrapolation of the linear region to the energy axis indicated a direct band gap of 1.65 eV (Fig. 3). The bandgap value is lower than that observed by Hus et al. [10].

Surface morphology of the films was studied using an atomic force microscope. It is observed that the grain size increased with increase of substrate temperature (Fig. 4). The grain size increased from 15 to 30 nm as the substrate temperature increased. The grain size is also observed to increase with increase of substrate temperature.

The XPS spectra of the CdSe films deposited at 300 °C and post heated at 500 and 550 °C are shown in Figs. 5a and b for the

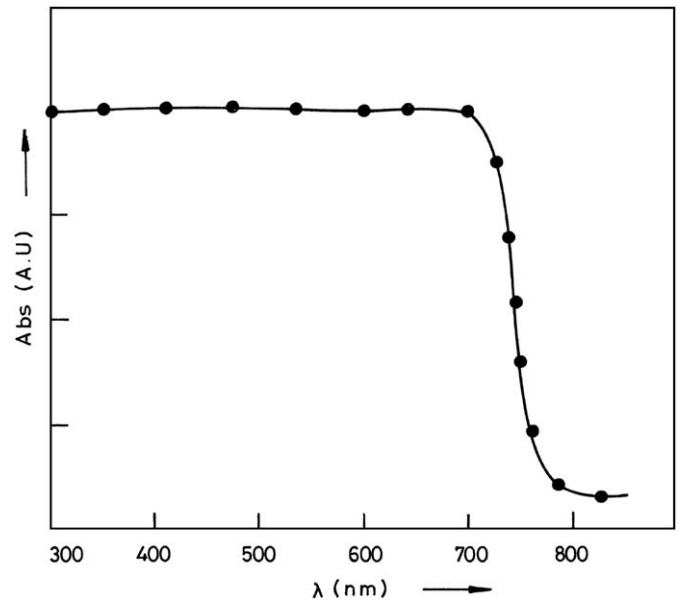


Fig. 2. Absorbance spectrum of CdSe films deposited at a substrate temperature of 300 °C.

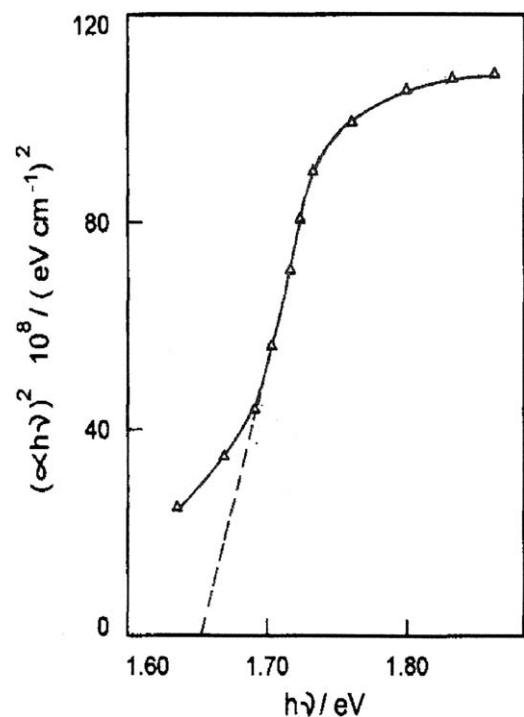


Fig. 3. $(\alpha h\nu)^2$ vs $h\nu$ plot of the CdSe films deposited at a substrate temperature of 300 °C.

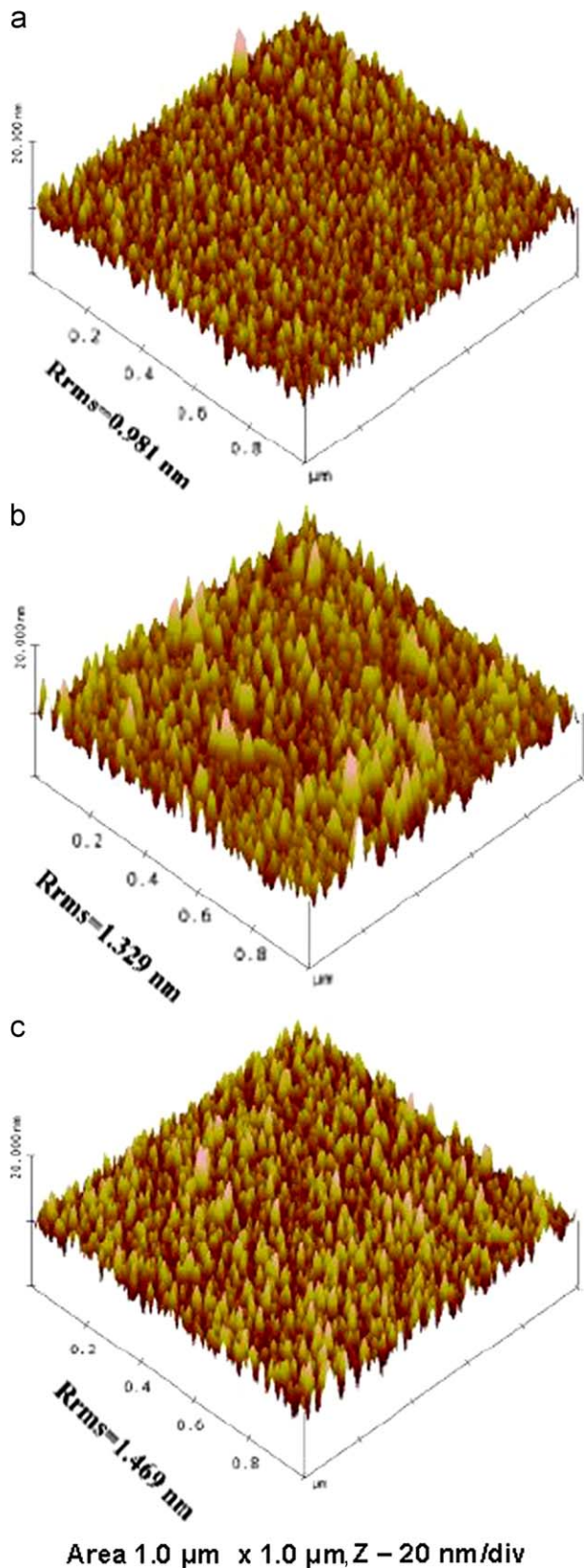


Fig. 4. Atomic force micrograph of CdSe films deposited at different substrate temperatures: (a) 100 °C ($R_a = 1.04$ nm), (b) 200 °C ($R_a = 2.43$ nm) and (c) 300 °C ($R_a = 5.45$ nm).

binding energies of the Cd ($3d_{5/2}$ and $3d_{3/2}$) and Se ($3d_{5/2}$ and $3d_{3/2}$) level. The films were washed with triple distilled water after heat treatment to remove any SeO_2 formed during the heat

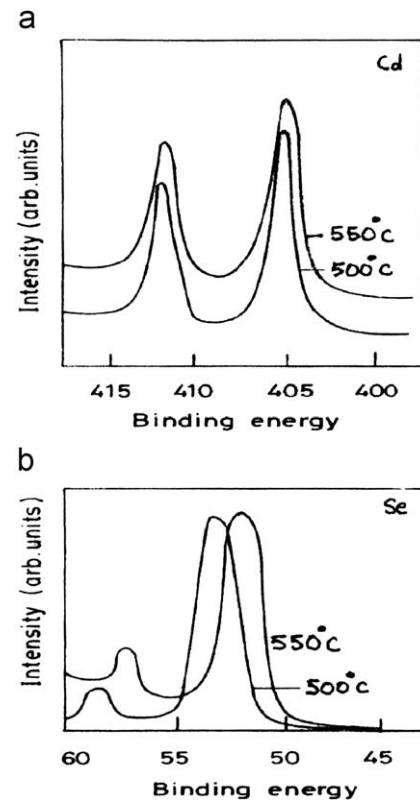


Fig. 5. XPS spectra of Cd and Se in CdSe films deposited at 300 °C and annealed in air.

treatment. After annealing the area under the selenium binding energy curves decreases indicating a small amount of loss of selenium upon evaporation from the sample due to heat treatment. As shown in Fig. 5a, the peak energy levels associated with Cd ($3d_{5/2}$ and $3d_{3/2}$) appeared at 405 and 411.7 eV, respectively, which are in good agreement with the literature [17]. Fig. 5b shows the binding energies of the Se ($3d_{5/2}$ and $3d_{3/2}$) levels at 53.9 and 59.2 eV, respectively. The selenium binding energies shift to lower energies after annealing due to loss of selenium by evaporation.

Fig. 6 shows the variation of photosensitivity of the films with intensity of illumination for the cells prepared by using the powder synthesized in the laboratory. The photosensitivity (S) was calculated using the equation

$$S = (R_D - R_L) / R_L \quad (1)$$

where R_L is the resistance under illumination, and R_D is the resistance under dark conditions.

It is observed from the figure that as the intensity of illumination increases, the corresponding photosensitivity also increases. Of all the annealing temperatures, the cells prepared with the films annealed at 550 °C exhibited maximum photosensitivity. The dependence of photosensitivity on light intensity at room temperature can be described in terms of the oxygen absorption effects at high annealing temperature. The thermal release of oxygen from the surface is the possible mechanism, which is always dominant for cells annealed in argon containing ppm of oxygen and hence both the photo and dark conductivity are increased [18]. The increase in photosensitivity may be due to the creation of opposite type of carriers in the n-type CdSe, as oxygen acts here as an acceptor impurity. Similar behavior has also been observed in CdSe photocells. Since the films annealed at 550 °C exhibited maximum photosensitivity, further studies were made only on these films.

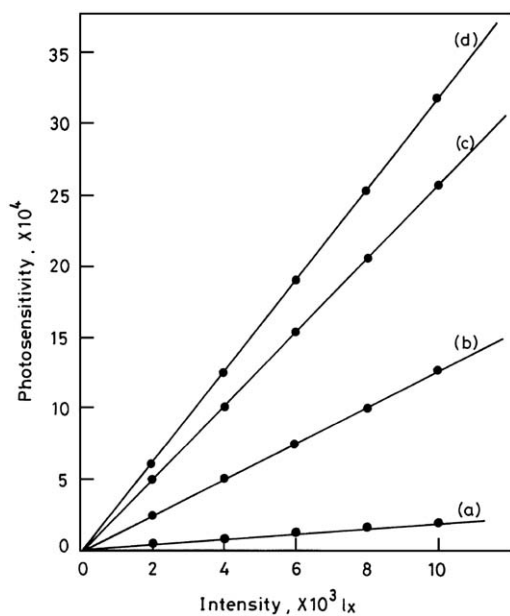


Fig. 6. Dependence of photosensitivity on illumination intensity for undoped CdSe films deposited at 300 °C and annealed in air at different temperatures: (a) 450 °C, (b) 500 °C, (c) 525 °C and (d) 550 °C.

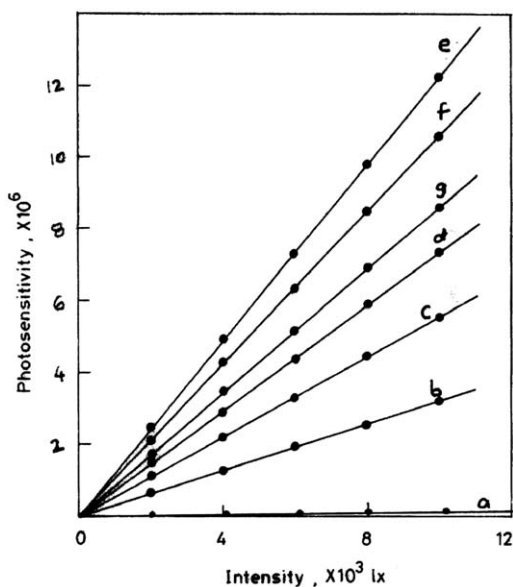


Fig. 7. Dependence of photosensitivity on illumination intensity for copper doped CdSe films deposited at 300 °C and annealed in air at 550 °C doped with different concentrations of copper: (a) 0.00 M, (b) 0.001 M, (c) 0.003 M, (d) 0.005 M, (e) 0.007 M, (f) 0.009 M and (g) 0.011 M.

Fig. 7 represents the plots of illumination intensity vs photosensitivity for all the cells doped with 0.001, 0.003, 0.005, 0.007, 0.009 and 0.011 M of copper. Similar to the undoped cells, the photosensitivity increases as the intensity of illumination increases. The magnitude of the photosensitivity is increased by two orders when compared to the undoped cells. Also, it is observed from the figure, as the copper concentration increases for a particular intensity and for a particular annealing temperature, the corresponding photosensitivity increases and it reaches a maximum when the copper concentration is 0.007 M and then decreases.

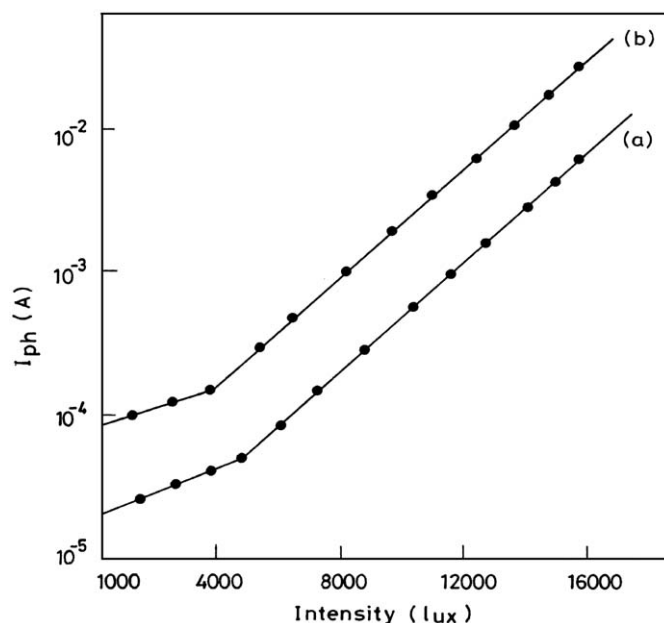


Fig. 8. Variation of photocurrent with illumination intensity for CdSe films (a) undoped and (b) doped with copper (0.007 M).

The incorporation of copper impurity in the CdSe films decreased the dark conductivity. Due to the dual nature of Cu impurities, the holes and electrons may recombine with the majority carriers under illumination thereby increasing the photosensitivity of the cell. In fact, studies of copper diffusion in CdS and CdSe [19] have shown that copper can act both as an acceptor and as a donor depending on whether it occupies substitution of interstitial sites in the lattice. The acceptor dominant behavior of copper arises when the number of copper ions on cadmium substitutional sites is larger than the number of atoms in the interstitial positions. It is clear from the results observed here that in the II–VI semiconductor compounds, copper is associated with photoconductivity sensitizing centers.

Copper (Cu⁺) centers are situated at 0.6 eV above the valence band as reported by Tyurn et al. [20]. The maximum photosensitivity is observed for the doping concentration of 0.007 M. AAS analysis of the copper concentration corresponding to this particular doping revealed the presence of 405 ppm of copper. This particular concentration corresponds to an acceptor to donor ratio around unity. For other concentrations of copper doping this ratio varies and hence photosensitivity decreases. The acceptor dominant behavior of copper arises when the number of copper ions on cadmium substitutional sites is larger than the number of atoms in the interstitial positions. Thus to fix the acceptor and donor concentrations as required above, the total donor concentration must be determined and a distinction between electrically active impurities and crystal defects as a function of processing variables must be made.

Fig. 8 shows the variation in the photocurrent with illumination for both the undoped and doped cells. As discussed earlier, the high photosensitivity associated with CdSe arises due to the presence of compensated acceptors, which act as sensitizing centers. As the excitation intensity is increased, these centers become more active and the photosensitivity sharply increases at some region of excitation. It is observed from the figure that up to 5000 lux, the photocurrent varies linearly with illumination, becoming super-linear above this intensity. But for the doped cells, linearity is observed up to 4000 lux and above this intensity super linearity is observed. The super linearity arises from the conversion of hole traps into recombination centers

Table 3
SNR of the CdSe films deposited at different substrate temperatures.

Substrate temperature (°C)	SNR
30	30
100	60
200	110
300	160

[Bias voltage: 170 V].

Table 4
SNR of the CdSe films deposited at 300 °C substrate temperature and doped with copper of different concentrations.

Concentration (ppm)	SNR
30	80
50	100
70	150
100	225

[Bias voltage: 170 V].

when the hole quasi-Fermi level moves towards the valence band with an increase in light intensity. These recombination centers, which have higher capture cross sections for the holes than electrons, in conjunction with another set of recombination centers with equal capture cross sections for both the carriers, decrease the lifetime of the holes thereby increasing the lifetime of the electrons. While the hole traps are being converted into recombination centers, the electron lifetime is continuously increasing and the photocurrent varies super linearly with increasing light intensity [21]. The transition from linearity to super linearity occurs when the hole demarcation level is at the level of the recombination centers with equal capturing cross section. Similar results were observed in sprayed [22], vacuum evaporated [23] and single crystal CdSe [24]. The super linearity in CdSe occurs only when the Fermi level varies between 0.3 and 0.6 eV from the conduction band. Also it is reported [25] that the small time constants of highly photosensitive films have been attributed to the super linearity of CdSe at higher intensity of illumination.

Tables 3 and 4 present the signal to noise ratio of the undoped CdSe films deposited at different substrate temperatures and Cu

doped films, respectively. It is observed that the SNR is found to increase gradually as the bias voltage increases and is found to be maximum for the films deposited at a substrate temperature of 300 °C. For the doped samples, SNR is maximum for a doping of 900 ppm of Cu. The SNR is higher for the doped films compared to undoped films.

4. Conclusion

The results obtained in this investigation clearly indicate that CdSe films exhibiting good photoconductive response and with high signal to noise ratio can easily be obtained by the electron beam evaporation technique. CdSe films with direct band gap of 1.65 eV can easily be obtained.

References

- [1] G. Hodes, A. Albu-Yaron, A. Decker, P. Motisuke, *Phys. Rev.* 36B (1987) 4215.
- [2] Y. Golan, L. Margulis, I. Rubenstein, G. Hodes, *Langmuir* 8 (1992) 749.
- [3] A.H. Mahmoud, *Cryst. Res. Tech.* 25 (1990) 1147.
- [4] K.C. Sathyalatha, S. Uthanna, P. Jayarama Reddy, *Thin Solid Films* 174 (1989) 233.
- [5] H. Padmanabhasarma, V. Subramanian, V. Rangarajan, K.R. Murali, *Bull. Mater. Sci.* 18 (1995) 875.
- [6] D. Hahn, K.K. Mishra, K.K. Rajeshwar, *J. Electrochem. Soc.* 138 (1991) 100.
- [7] K.N. Shreekanthan, B.V. Rajendra, V.B. Kasturi, G.K. Shivakumar, *Cryst. Res. Tech.* 38 (2003) 30.
- [8] A.O. Oduor, R.D. Gould, *Thin Solid Films* 270 (1995) 387.
- [9] K.N. Shreekanthan, B.V. Rajendra, V.B. Kasturi, G.K. Shivakumar, *Cryst. Res. Tech.* 38 (2003) 30.
- [10] S.M. Hus, M. Parlak, *J. Phys. D* 41 (2008) 035405, (8pp.).
- [11] C. Kaito, Y. Saito, *J. Cryst. Growth* 99 (1990) 743.
- [12] K. Reichelt, X. Jiang, *Thin Solid Films* 191 (1990) 91.
- [13] K.L. Chopra, *Thin Film Phenomena*, McGraw Hill, New York, London, 1969, p. 272.
- [14] V. Kumar, B.S.R. Sastry, *Cryst. Res. Tech.* 36 (2001) 565.
- [15] G. Perna, V. Capozzi, M.C. Plantamura, A. Minafra, P.F. Biagi, S. Orlando, V. Marotta, A. Giardini, *Appl. Surf. Sci.* 186 (2002) 521.
- [16] P.K.R. Kalita, B.K. Sharma, D.L. Das, *Bull. Mater. Sci.* 23 (2000) 313.
- [17] O. Savadogo, K.C. Mandal, *Mater. Chem. Phys.* 31 (1992) 301.
- [18] H. Shear, E.A. Hilton, *J. Electrochem. Soc.* 112 (1965) 997.
- [19] A. Rose, *Concepts of Photoconductivity and Allied Problems*, Wiley, NY, 1963.
- [20] L.I. Tyurn, Yu.A. Varvas, *Tr. Tallin, Politekh. Inst. Ser. A* 236 (1966) 39.
- [21] H. Okhimura, Y. Sakai, *Japan. J. Appl. Phys.* 7 (1968) 731.
- [22] A.K. Raturi, R. Thangaraj, P. Rajaram, B.B. Tripathi, O.P. Agnihotri, *Thin Solid Films* 106 (1983) 257.
- [23] R.H. Bube, in: *Proceeding Conference, Photoconductivity*, Atlanta, 1954.
- [24] A.K. Raturi, R. Thangaraj, P. Rajaram, B.B. Tripathi, O.P. Agnihotri, *Thin Solid Films* 91 (1982) 55.
- [25] C.M. Lampert, R. Mark, *Current Injection in Solids*, Academic Press, NY, 1970.